Discover Sustainability

RESEARCH Open Access

Biomethane as a promising renewable carbon feedstock for the synthesis of zeolite templated carbons for hydrogen storage application

Keaoleboga Mosupi[1], Xoliswa Dyosiba[2], Henrietta W. Langmi[1*] and Nicholas M. Musyoka[3*]

*Correspondence:
Henrietta W. Langmi
henrietta.langmi@up.ac.za
Nicholas M. Musyoka
nicholas.musyoka@nottingham.edu.cn
[1]Department of Chemistry, University of Pretoria, Hatfield 0002, South Africa
[2]Department of Chemical Engineering, University of Pretoria, Hatfield 0002, South Africa
[3]Nottingham Ningbo China Beacons of Excellence Research and Innovation Institute, University of Nottingham Ningbo China, Ningbo 315100, People's Republic of China

Abstract

Biogas, generated through the anaerobic digestion of organic matter, is an attractive renewable energy source due to its continuous production and utilisation cycle. Rising concerns about the environmental impact of fossil fuel-derived energy have sparked interest in developing sustainable energy alternatives. Consequently, considerable research efforts have been directed towards biogas valorisation, particularly its main component, methane (CH_4). This is achieved by converting raw or upgraded biogas into high-value products, such as Zeolite-templated carbons (ZTCs), and concurrently producing cleaner hydrogen gas. ZTCs are highly ordered porous structures that exhibit high surface areas, uniform pore size distributions, and large pore volumes, rendering them attractive for various applications. These applications include gas storage, CO_2 capture, supercapacitors and batteries. In this study, we focused on the utilisation of simulated biogas (CH_4 and CO_2 mixture) and pure CH_4 (in this case, simulated 'biomethane') for the synthesis of zeolite-templated carbons (ZTCS). When CH_4 was utilised on both the one-step and two-step processes, the obtained ZTCs had higher surface area and hydrogen (H_2) adsorption. The highest surface area obtained was 2974 m^2/g, while the best H_2 storage capacity, at 1 bar, was 2.77 wt%. Structural (XRD) and morphological (SEM and TEM) characterisations were found to be indistinguishable from those of the samples obtained when fossil-derived ethylene was used as a carbon source. Unfortunately, ZTCs were not obtained when simulated biogas was used as a carbon source, due to the zeolite having a greater affinity towards CO_2 than CH_4, primarily because of the large quadrupole moment of CO_2. This study has demonstrated that a sustainable source of carbonaceous feedstock, such as biogas-derived 'biomethane', can be converted into value-added products (ZTCs), thereby creating additional economic opportunities for industries within the biogas sector.

Keywords Biogas, Biomethane, Zeolite 13X, Zeolite templated carbons, Hydrogen adsorption, Chemical vapour deposition

1 Introduction

Raw biogas is a product of anaerobic decomposition of organic matter under controlled temperature, acidity, and moisture conditions. Various types of organic feedstock can be used for the production of biogas, e.g., municipal solid waste, animal manure, algae, kitchen waste, crop straws and leaves, among others [1, 2]. The main constituents of biogas are CH_4 and CO_2 together with traces of H_2S, H_2, N_2 CO, NH_3, volatile organic compounds (VOCs), siloxanes and some water vapour [3]. Raw biogas can be used as a fuel for gas turbines, domestic cooking, and even as a raw material in the chemical industry [4]. The use of biogas is mainly dependent on the high concentration of CH_4, which has a higher calorific value than the other constituents [5]. The relatively higher content of CO_2 and N_2 are known to lower the calorific value of biogas. In this case, removing unwanted compounds such as VOCs, siloxanes, CO, and NH_3, regarded as "biogas cleaning", is the first step to biogas treatment. It is then followed by biogas upgrading, which mainly focuses on removing CO_2 [6]. The recovered CO_2 can be used as a precursor for producing chemicals such as methanol, dimethyl carbonate, and methane, among others. While purifying raw biogas to yield biomethane incurs some energy-related costs, this process is already widely embedded into existing waste-to-energy infrastructures and remains essential for numerous applications, including grid injection and fuel-grade methane production. Importantly, this study leverages this existing stream, thus aligning with circular economy principles. Methane serves as a model carbon precursor due to its well-defined molecular structure, clean decomposition behaviour, and high carbon yield when subjected to chemical vapour deposition (CVD) within zeolitic frameworks. This enables precise control over carbon growth and replication of the zeolite pore structure. Furthermore, the resulting biomethane-derived ZTCs exhibit favourable structural characteristics, such as hierarchical porosity, high surface area, and a well-defined micropore network, that directly contribute to enhanced hydrogen uptake performance. These features distinguish them from ZTCs derived from conventional precursors, supporting their suitability for energy storage applications. Nevertheless, we agree that a comprehensive life cycle analysis or energy balance analysis would further contextualise this trade-off and propose it as an important direction for future work. We further acknowledge that methane has been widely utilised as a fuel due to its high calorific value; however, its conversion into solid carbons offers certain strategic advantages that justify exploring alternative use pathways. In this case, methane cracking offers dual benefits related to the production of low-carbon "turquoise" hydrogen production and the concurrent generation of higher-value carbonaceous materials (in this case, ZTCs). This alternative pathway is of particular importance, especially where biomethane sources are localised, rendering direct grid injection an inefficient option. While methane has an upper hand as an energy carrier, its utilisation as a carbon feedstock presents a complementary strategy that simultaneously supports cleaner hydrogen production and carbon valorisation.

Several studies have conducted research on adsorption of CH_4 on zeolites due to high polarizability of the gas. Mofarahi and Bakhtyari tested the adsorption of pure CH_4 on zeolite 13X at 273, 283, 303, 323, and 343 K and pressures up to 10 bar. The zeolite adsorbed 3.09, 2.95, 2.70, 2.30 and 1.87 mol/kg at respective temperatures [7]. Cavenati et al. performed adsorption of CH_4, CO_2, and N_2 on zeolite 13X which was measured in the pressure range 0 to 50 bar and temperatures of 298, 308, and 323 K. CH_4 displayed

maximum adsorption of 5.71, 5.23 and 4.83 mol/kg at respective temperatures [8]. Zeolite 13X beads were tested for CO_2 and CH_4 adsorption equilibrium, The adsorbed amount of CH_4 was 1.2 mol/kg and CO_2 around 5.2 mol/kg, respectively, at 313 K and 4 bar [9]. Although zeolites have favourable adsorption of CH_4 at low pressures due to their microporosity, their structural rigidity is a limiting factor in high-performance storage systems. The use of CH_4 as a precursor for synthesis of zeolite-templated carbons (ZTCs) provides an alternative that has similar micropore environment as zeolites but with improved surface area, pore volume and adsorption behaviour.

Amongst the many existing soft and hard templated carbons, ZTCs are an attractive group of porous sorbents [10, 11]. ZTCs are produced using zeolite as a nanocasting template utilising a gaseous or liquid carbonaceous feedstock. Various types of zeolites can be utilised for the synthesis of ZTCs [12]. On the other hand, ethylene has been preferred as an ideal gaseous feedstock, and furfural alcohol is the preferred liquid feedstock for impregnating zeolite templates [13]. ZTCs are known to be utilised in many applications, such as hydrogen storage, carbon capture, methane storage, and gas separation, among others [14]. There are two approaches that can be followed for the synthesis of ZTCs, i.e., a one-step process which involves impregnation of zeolite template with gaseous carbon source whereas a two-step process involves impregnation of the template with liquid carbon feedstock followed by gaseous feedstock [15]. Noteworthy, previous studies have reported that parameters, such as the type of carbonaceous precursor, manner of carbon precursor impregnation into the zeolite pores, and conditions for carbonisation can have effects on properties of the resulting ZTCs [13, 16, 17]. These resulting ZTC materials are earmarked for energy-related applications.

The need for renewable energy that is efficient, and cost effective has increased globally, enabled by the need to circumvent the effects of climate change. These reasons have significantly induced research in areas of energy production, storage, distribution and consumer. At the centre of these discussions is the use of hydrogen as a green, efficient energy carrier. Hydrogen, a low-density gas under ambient conditions with an astounding gravimetric energy density that is almost three times that of regular gasoline, has wee-known challenges in terms of its storage. Several storage methods have been explored, such as high-pressure storage, cryogenic liquid storage, and adsorption or absorption in materials. Although high pressure and cryogenic storage offer high gravimetric capacities, they are limited by high energy demands, safety issues, and additional infrastructure requirements. Physisorption is of particular interest due to high reversibility, fast kinetics and cyclability. Hydrogen storage by physisorption requires nanomaterials with a narrow pore size range (< 2 nm) and high specific surface areas (> 1500 m^2/g), where hydrogen density is improved compared to the bulk gas phase at the same temperature and pressure. Of interest are ZTCs, as they are considered to display high hydrogen capacity due to their high surface area, distinctive pore structure, chemical stability, and cost-effectiveness (owing to the use of a renewable resource, biomethane). These properties enhance hydrogen adsorption by inducing potential energy fields from pore walls, thus allowing adsorption at low pressures and liquid nitrogen temperatures (77 K).

Several researchers have investigated the hydrogen storage capacity of ZTCs at various pressures and temperatures. For example, three ZTCs were prepared using three different zeolites, which displayed surface areas of 1691, 2964 and 3591 m^2/g and their

corresponding hydrogen uptake of 18.5, 26.1 and 28.6 mol/kg at 77 K [18]. Musyoka et al. performed a comparative study of ZTCs derived from commercial zeolite X and coal fly ash-derived zeolite X. ZTC derived from commercial zeolite displayed hydrogen uptake of 2.4 wt% while ZTCs from fly ash zeolite showed hydrogen uptake of 1.2 wt% at 77 K and 1 bar [16]. Annamalai et al. further explored electrospinning as a shaping technique for ZTCs; the electrospun ZTC composite material displayed a hydrogen uptake of 1.83 wt% at 77 K and 1 bar, which was 76% of the powder material [19].

Other gas adsorption studies, such as methane uptake, have been conducted to demonstrate the potential of ZTCs as gas adsorbents. ZTCs prepared using two different zeolite structures, i.e., BEA and FAU, were tested for CH_4 adsorption. The ZTCs prepared from BEA zeolite, displayed total CH_4 uptake of 16.39 mol/kg at 65 bar [20]. Stadie et al. studied the adsorption of CH_4 on ZTCs, the ZTC-3 material displayed CH_4 adsorption of 22.1 mol/kg (26.2wt%) at 47 bar and 238 K [21]. ZTCs prepared using zeolite beta and acetylene as carbon precursor displayed a high methane gravimetric uptake of up to 8.0 wt% at 298 K and 35 bar, which was far greater than the parent zeolite (1.5 wt%) at similar conditions [22]. A high surface area (1562 m^2/g) microporous carbons prepared using glucose and zeolite NaY showed adsorption of 6.89 mol/kg (9.9 wt%) at 300 K and 35 bar.

To the best of our knowledge, there are no studies that have reported on the use of biogas as a carbon source for the synthesis of ZTCs. In this work, we report on the use of simulated biogas, i.e., a mixture of CO_2 and CH_4, based on their average composition in biogas. We further compare the obtained product from simulated biogas to ZTCs obtained using pure methane (supposed to be obtained from upgraded biogas). The study contributes to the circular economy through the potential use of sustainable feedstock (biomethane) rather than the reliance on fossil-derived gas feedstocks.

2 Materials and experimental procedure

Zeolite X was purchased from Sigma Aldrich, whereas ethylene, methane and argon were purchased from Air Products. The chemicals and reagents used in this study were used without further purification. For the synthesis of ZTCs using simulated biogas, commercial powdered zeolite 13 × (5 g) was dried under vacuum at 200 °C for 12 h to remove any trapped or adsorbed water molecules from the zeolite cavities. The sample was packed in a sample boat and placed in a tube furnace and the temperature was increased to 900 °C (heating rate of 10 °C/min) and held at that temperature for 3 h. Thereafter, a mixture of CH_4 and CO_2 (ratios 2:3, 4:1, 2.3:1) gas was passed through the tube furnace for 3 h. For the synthesis of ZTC using methane, the above procedure was repeated, but a mixture of CH_4 and Ar (ratio 1:1) gas was passed through the tube furnace where chemical vapour deposition (CVD) and carbonisation of CH_4 took place for 3 h. To remove the inorganic zeolite structure from the carbons, the sample was washed with 20% hydrofluoric acid (40 mL) for 3 h, and thereafter, the sample was filtered and washed with deionised water (1000 mL). The sample was washed via reflux in 20% hydrochloric acid at 70 °C for 24 h. The recovered ZTC was filtered and washed with deionised water (1 L) and dried in a conventional oven at 90 °C for 12 h. The procedure for the synthesis of ZTC following the two-step approach was as follows: Furfural alcohol (17 mL) was firstly impregnated into 5 g of dried zeolite for 24 h. The composite sample was filtered and then air-dried at ambient temperature for 3 h after being rinsed with ethanol (1 mL). The sample was

then dispersed in a quartz boat put into the tube furnace for the CVD procedure. The sample was first polymerised at 80 °C for 24 h under argon gas, then again at 150 °C for 8 h. Temperature was then increased to 900 °C. Thereafter, methane was introduced into the tube furnace for 3 h. The sample then underwent the detemplation process following similar procedure as reported earlier. For comparison purposes the experimental procedure was repeated using ethylene as a carbon source. The samples obtained from methane were coded as ZTCmt and FAZTCmt whereas those obtained from ethylene were called ZTCet and FAZTCet.

2.1 Characterisation

Powder X-Ray Diffraction (PXRD) analyses were conducted using Rigaku Ultima IV diffractometer using Ni-filtered Cu-Kα radiation (0.154 nm) in the range of $2\theta = 1–90°$ at a scanning rate of 0.1°s – 1. Morphological characteristics were examined under a JEOL-JSM 7500 F scanning electron microscope. High-resolution micrographs of ZTC samples were captured using a JEOL-Jem 2100 model transmission electron microscope (TEM). Using the Micromeritics(R) ASAP 2020 HD, BET surface area measurements were conducted at liquid N_2 temperature (77 K) and relative pressures (P/P_0) ranging from 0 to 1. After outgassing at 200 °C under vacuum for the whole night, N_2 adsorption-desorption isotherms were obtained, and the linear portion of the N_2 isotherms was used as the basis for obtaining the BET surface areas. Pore size distribution plots and pore volumes were derived using the Horvath–Kawazoe (HK) model. H_2 adsorption isotherms at 77 K and up to 1 bar, were also measured on the Micromeritics(R) ASAP 2020 HD instrument. All gas sorption isotherms were obtained using ultra-high purity grade (99.999%) gases. Thermal stability of the prepared samples was determined using TGA instrument (TA instruments, Q500 model). In this case, samples were loaded onto alumina crucibles and measurements were conducted under air at a heating rate of 10 °C/min at a temperature range of 0 °C to 1000 °C.

3 Results and discussions

3.1 Structural analysis

The comparative XRD patterns of samples obtained when using ethylene and pure methane as carbonaceous feedstock are represented in Fig. 1. All the samples, whether synthesised using the one or two-step method, displayed a dominant sharp peak at $2\theta = 6.3°$ which originated from the (111) structural regularity of FAU zeolite, which was also previously observed [16]. This peak denotes the maintenance of the zeolite-like structural regularity. Two broad peaks at around $2\theta = 23°$and $2\theta = 42°$, with the ZTCet and ZTCmt samples having a more pronounced appearance, indicate the existence of graphitic carbons, such as graphene layers, nano-graphene networks, or some graphene stacking. These two peaks could be indexed as the 002 and 101 planes of the graphitic carbons. Unfortunately, ZTCs were not obtained when simulated biogas was used as a carbon source due to zeolite having a greater affinity towards CO_2 than CH_4 because of the large quadrupole moment of CO_2. The quadrupole moment has a strong attraction towards the electrostatic field of the cationic sites thus greater selectivity and higher adsorption capacity [23]. Pour et al. studied clinoptilolite and zeolite 13X ability to separate CO_2 from CH_4, and concluded that both materials have high affinity towards CO_2 due to the quadrupole moment of CO_2 molecules with the surface of adsorbents. CH_4

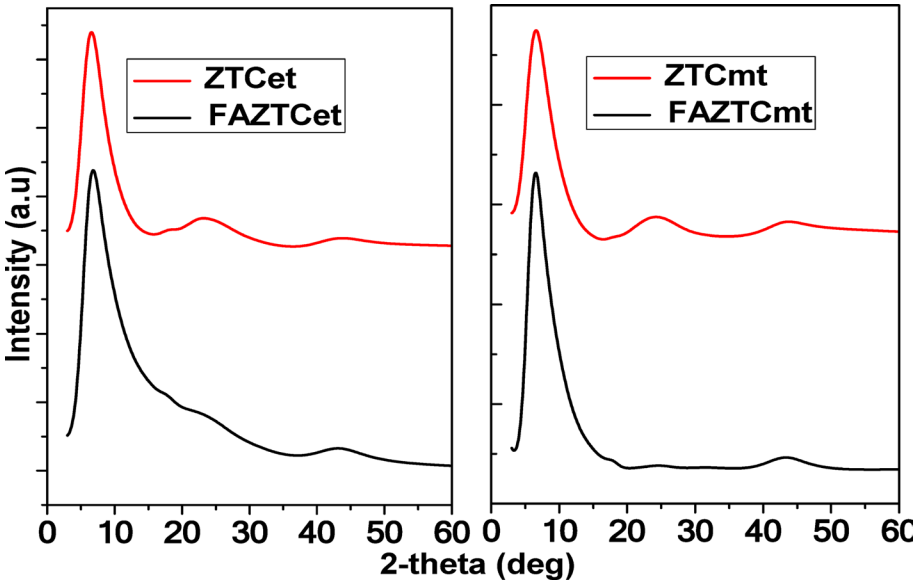

Fig. 1 X-ray diffraction pattern for ZTCet, FAZTCet, ZTCmt and FAZTCmt

is a non-polar molecule with no dipole and quadrupole moment, which results in weak interaction with zeolites [24]. The attraction of CO_2 towards zeolite 13X is supported by many other researchers [9, 25, 26]. It can then be concluded that the use of biogas as a carbon feedstock in the synthesis of ZTCs is not possible since zeolite 13X has preferential adsorption of CO_2 over CH_4 and CO_2 is thermally stable to be carbonised in the pores of the zeolite.

4 Morphological Analysis – Scanning electron microscopy (SEM)

SEM images presented in Fig. 2, confirmed morphological similarity between the zeolite and the carbon replicas. The octahedral pyramidal shape, which is associated with zeolite 13X, was observed on the templated carbons. The templated carbons (Fig. 2b, c, d, e) have a smooth surface which resembles that of the parent zeolite (Fig. 2a), and the results are in line with those reported by Kyotani et al. using zeolite Y [27].

5 Transmission electron microscopy

Representative transmission electron micrographs obtained for samples ZTCmt and FAZTCmt are presented in Fig. 3. It is noteworthy that the particles are free of any appreciable exterior layer, which eliminates the possibility of graphitisation caused by carbon deposited on the outside of the zeolite particle. The selected area diffraction pattern (SAED), which denotes scattering from an amorphous material, significantly contributed to the understanding of the ZTCs' amorphous nature.

5.1 Thermogravimetric analysis

Determination of the temperature at which materials decompose is of great importance for application purposes. Therefore, TGA analysis was conducted on the ZTCs, and the results are presented in Fig. 4. The weight loss observed at around 0 and 100 °C (~ 5%) can be attributed to the evaporation of water molecules trapped within the ZTCs pores. It was noted that the ZTCs are thermally stable up to 500 °C, after which there is a noticeable weight loss between 600 and 700 °C, as shown by TGA. This drastic weight

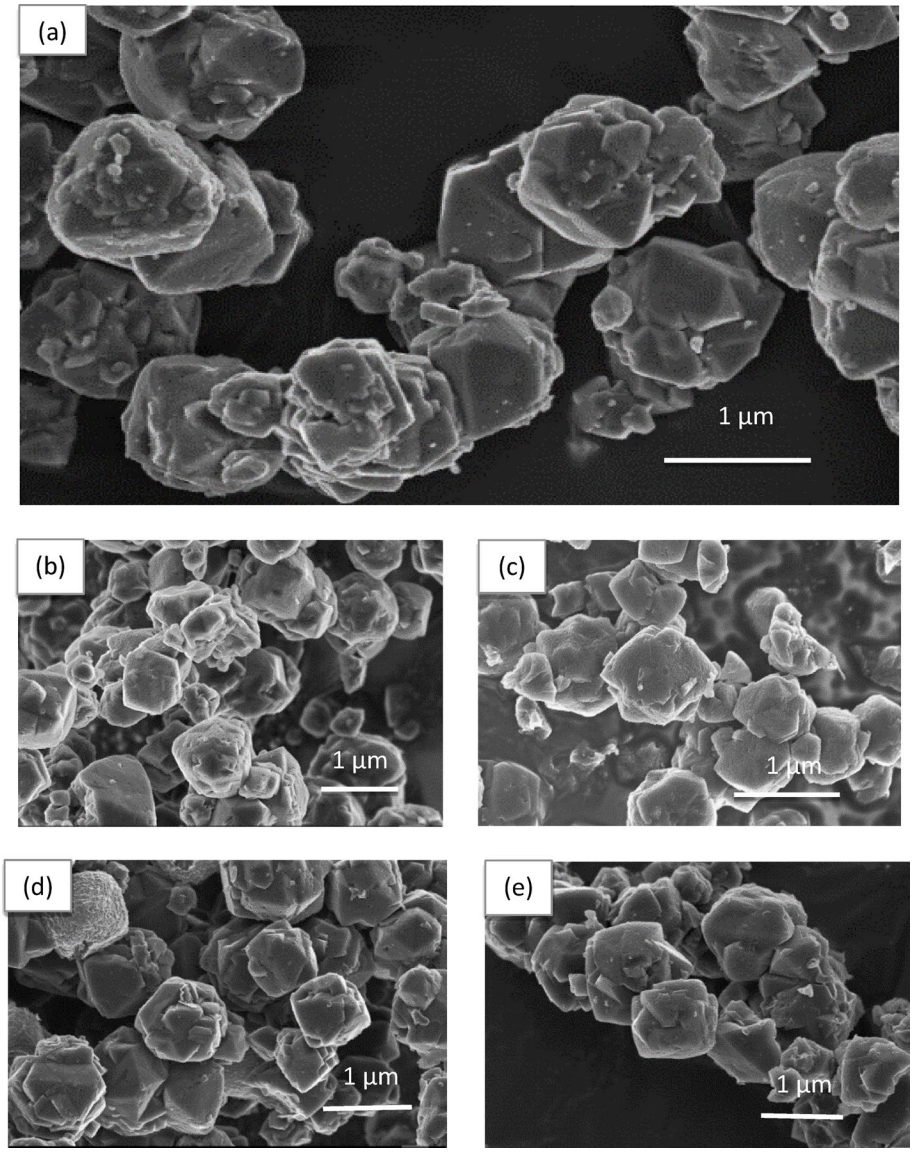

Fig. 2 SEM images of (**a**) Commercial Zeolite 13X (**b**) ZTCet (**c**) ZTCmt (**d**) FAZTCmt (**e**) FAZTCet

loss can be attributed to the carbon burn-off. The high thermal stability of these materials is further enhanced by the presence of graphitic carbons as indicated by PXRD at $2\theta = 23°$and $2\theta = 42°$. The complete loss of weight of the material indicates that the detemplation process was successful since no traces of the zeolite 13X were evident.

6 Raman spectroscopy

Raman spectroscopy is an important technique to understand the graphitic nature of the carbon material; it has the potential to differentiate between ordered and disordered carbons [28]. In this case, Raman spectrum can show the D-band, which represents the disordered carbons, and G-band is for the graphitic carbon [17]. Fig. 5 presents the Raman spectra of ZTCs synthesised using one- and two-step processes. As expected for sp^2-carbons, the spectrum of the one-step process showed the D band of ZTCet and ZTCmt at 1361 cm^{-1} and 1337 cm^{-1}, while the G band is located at 1603 cm^{-1} and 1595 cm^{-1}, respectively [14]. The two-step process shows the D band of FAZTCet and FAZTCmt

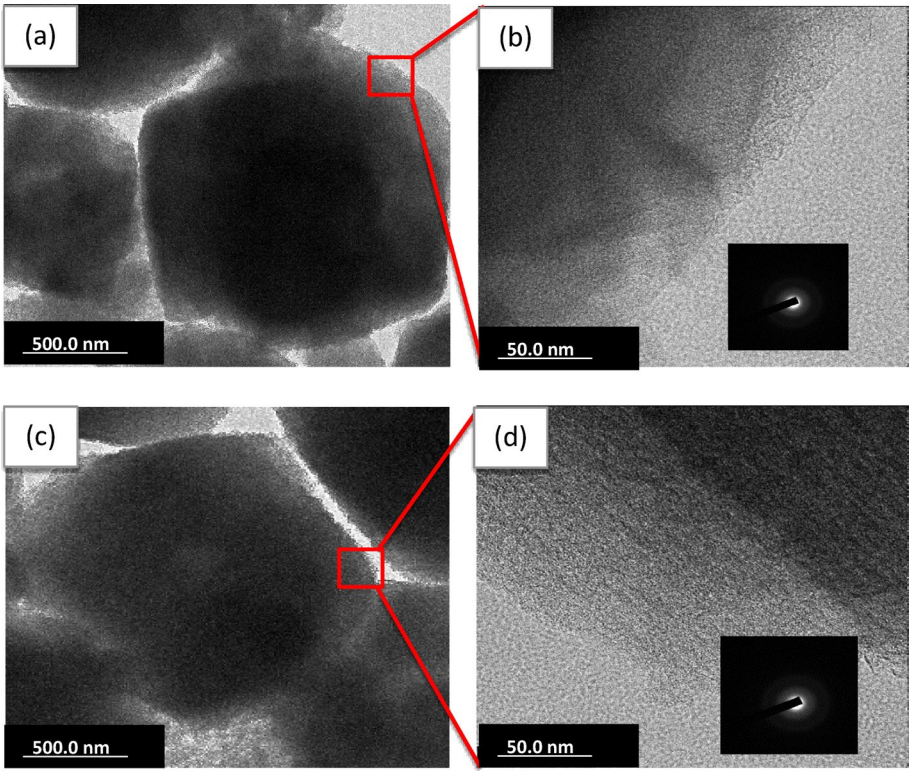

Fig. 3 TEM images of templated carbons (**a**) low resolution ZTCmt (**b**) high resolution ZTCmt (**c**) Low resolution FAZTCmt (**d**) High resolution FAZTCmt

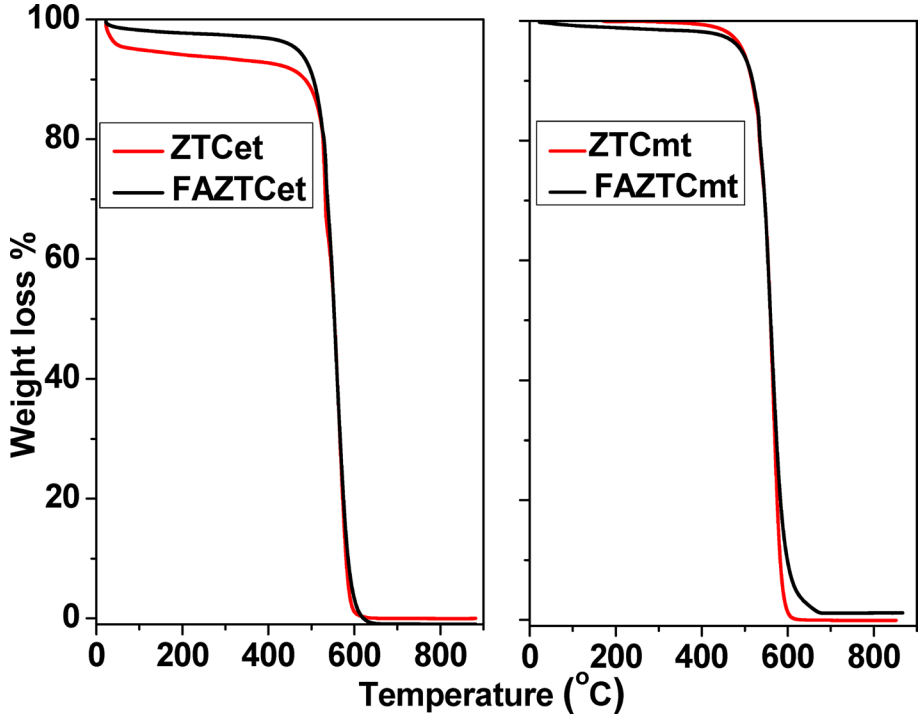

Fig. 4 Thermogravimetric analysis for ZTCet, FAZTCet, ZTCmt and FAZTCmt

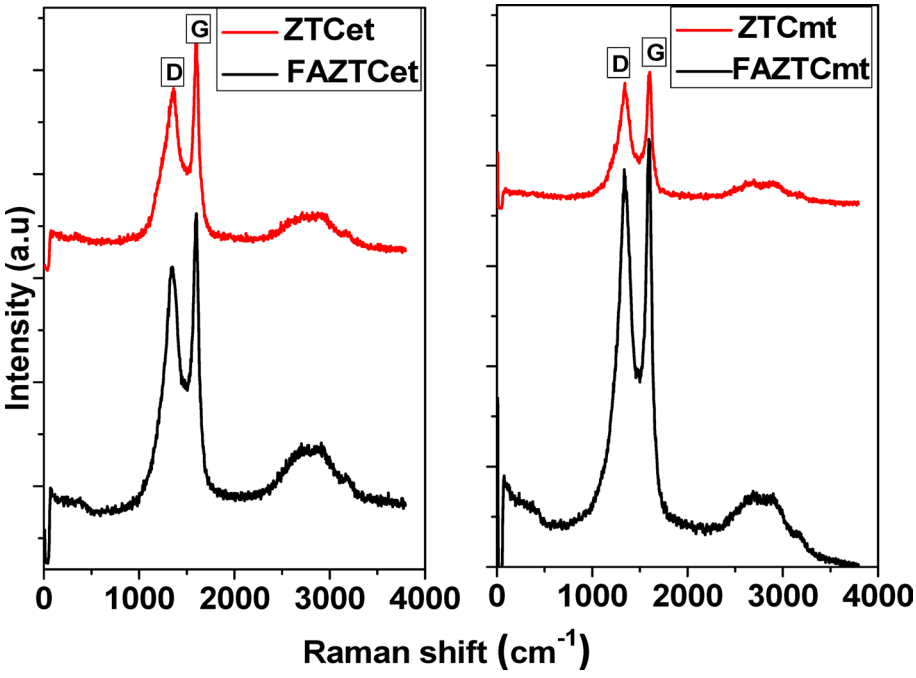

Fig. 5 Raman analysis for ZTCet, FAZTCet, ZTCmt and FAZTCmt

Table 1 Raman analysis data of ZTCet, ZTCmt, FAZTCet and FAZTCmt

Sample name	D Band	G Band	I_D/I_G
ZTCet	1361	1603	0.86
ZTCmt	1337	1595	0.95
FAZTCet	1349	1603	0.89
FAZTCmt	1341	1599	0.96

at 1349 cm^{-1} and 1341 cm^{-1}, respectively, while the G band is at 1603 cm^{-1} and 1599 cm^{-1}. In contrast to graphite, the ZTCs appear to be largely composed of nanometer-sized graphene sheets, as evidenced by the G bands' location, which is somewhat higher than that of graphene, and the strong intensity of the D bands relative to that of the G bands [29]. The broad bands observed between 2300 and 3300 cm^{-1} are attributed to the second order Raman scattering as a result of two-phonon process, are also in agreement with this interpretation [30]. The higher intensity ratio (ID/IG) of methane-based products as observed in Table 1, and proves that the high temperature affected the amorphous carbon by forming more defects. The intensity of the D band is almost equal to the G band on methane-derived ZTCs as compared to the ethylene-derived ZTCs; this suggests that methane-derived ZTCs are dominated by defects. The defects may be a result of the sp3-carbons, dangling bonds, presence of defective pores (diameter greater than 2.2 nm) and other types of defects [31].

7 Adsorption studies and physical properties

N_2 sorption isotherm at 77 K of both one- and two-step synthesis routes for ethylene and methane-derived ZTCs are presented in Fig. 6. A Combination of type I + IV isotherms was observed for all the obtained ZTCs, which is in line with IUPAC classification outlined by Thommes et al. [32] The isotherm combination of templated carbons has been observed by several other researchers [33–35]. The presence of micropores is

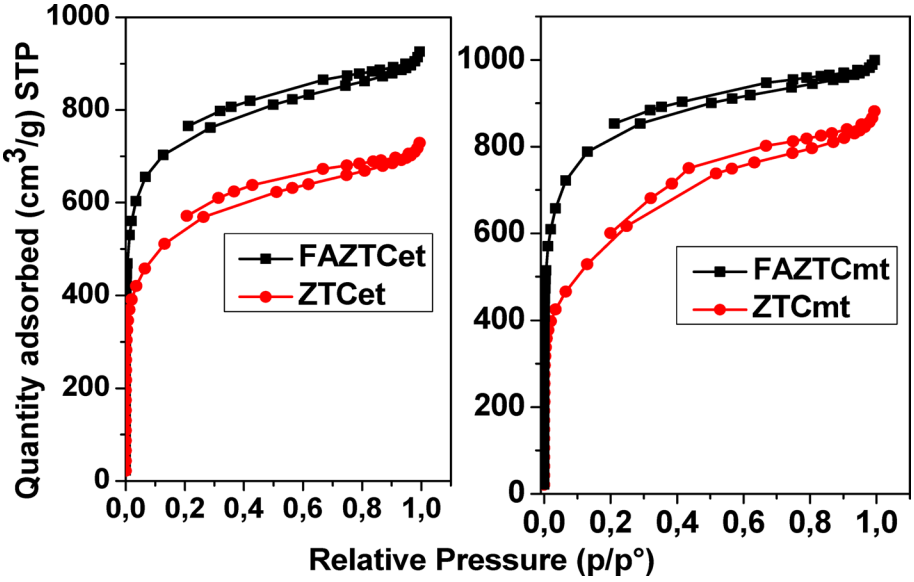

Fig. 6 N_2 sorption isotherms for ZTCet, FAZTCet, ZTCmt and FAZTCmt

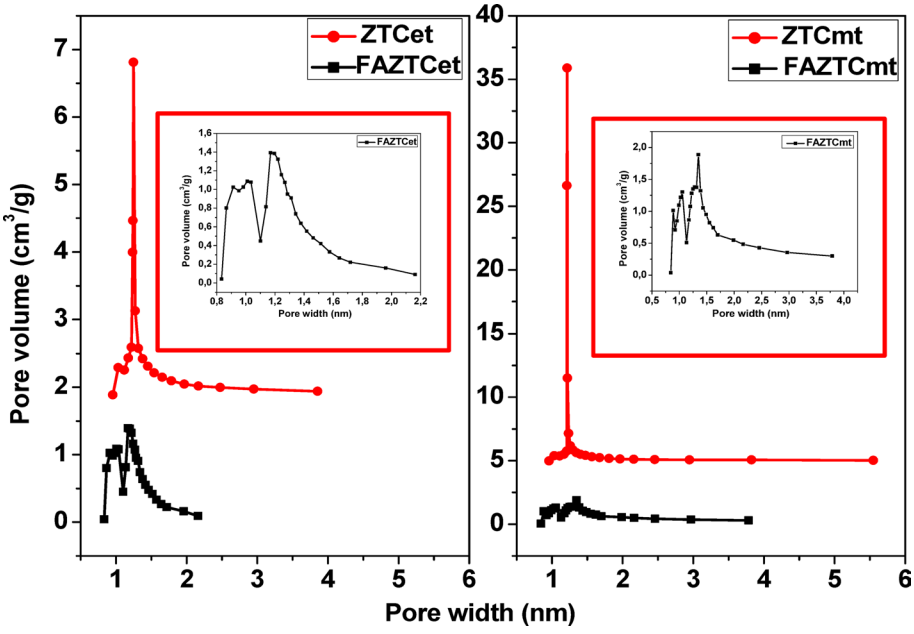

Fig. 7 Pore size distribution plot for ZTCet, FAZTCet, ZTCmt and FAZTCmt

evidenced by the sharp rise in N2 adsorption at the lower relative pressure (p/p0 < 0.1). Type IV isotherm characteristics are due to the presence of a broader pore size distribution, including narrow micropores (< ~ 1 nm) and narrow mesopores (< ~ 2.5 nm) (see Fig. 7). The presence of micropores in the prepared material can be an indication of the successful replication of the zeolitic structural ordering. This is further supported by the (111) planes displayed on the XRD pattern. The hysteresis loop (type H4, usually associated with micro-mesoporous carbons), which is caused by capillary condensation and indicates the presence of mesopores, occurs at approximately p/p0 >0.2 [32]. Mesoporosity may be caused by spaces between particles or by insufficient carbon filling of

Table 2 Textual properties and H_2 uptake capacities of ZTCmt, ZTCet, FAZTCmt, and FAZTCet

Sample name	BET Specific surface area (m^2/g)	Average Pore size (nm)	Total pore volume at p/p^o= 0.99 (cm^3/g)	H_2 uptake (wt%)
ZTCmt	2015	1.21	0.95	1.91
ZTCet	1850	1.24	0.79	1.88
FAZTCmt	2974	1.28	1.21	2.77
FAZTCet	2674	1.22	1.08	2.50

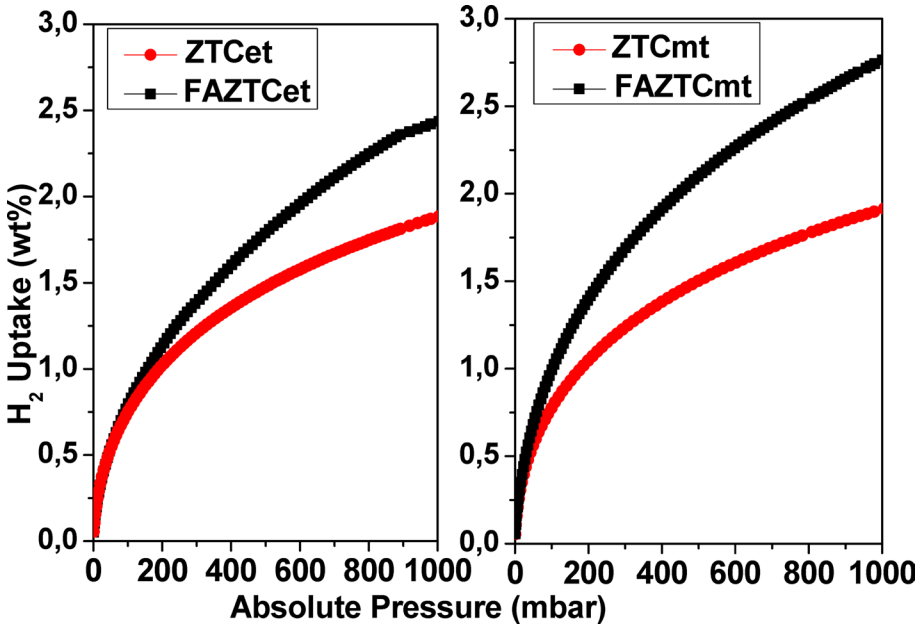

Fig. 8 H_2 uptake for ZTCet, FAZTCet, ZTCmt and FAZTCmt

zeolite micropores [33]. The isotherms are consistent with results from carbons made from zeolite templates that exhibit high degrees of structural organisation [34].

7.1 Pore size distribution

Figure 7 presents the pore size distribution plots (PSD) generated using the Horvath-Kawazoe (H-K) method. The PSD of the carbons appeared to be dominated by the pores at around 1.2 nm (the maximum values are recorded in Table 2) which is consistent with previous studies reported by Masika and Mokaya [35]. These findings agree with higher zeolite structural ordering, which does not possess pore sizes larger than 1.5 nm. The carbons obtained using methane had a narrow, sharp PSD, which shows that the carbons are highly porous. The pore splitting at the range 0.8–1.22 nm for the samples obtained from the two-step synthesis process may be as a result of ultramicropore filling of the zeolite pores during FA polymerisation and CVD process. The one-step synthesis method did not show this pore splitting which may be due to the inability of molecules to access ultramicropores.

7.2 Hydrogen sorption studies

The H_2 sorption isotherms of ZTCs, at 77 K and 1 bar, are presented in Fig. 8. The absence of the hysteresis loop suggests the complete reversibility of hydrogen adsorption.

It was noted that ZTCs can adsorb hydrogen at relatively high pressures since there is no saturation at 1 bar. Specific surface area, pore volume, and micropores of material are influential on the adsorption of hydrogen. The FAZTCmt, which has a higher surface area and pore volume, had a relatively high hydrogen storage capacity (2.77%) compared to FAZTCet (2.50%). The results obtained in this study are comparable to those reported by Cai et al. (6.1 wt% at 77 K and 20 bar). Although adsorption was performed at 20 bar, the amount adsorbed at low pressure regions (2 wt% at < 2 bar) is similar to that obtained in this study [36]. In another study, ZTCs from zeolite Y displayed a 2.4 wt% of hydrogen at 20 bar and 77 K, which is very similar to the values reported in this study [37]. An excess hydrogen uptake of 5 wt% was reported at 77 K and 20 bar [38]. The above-mentioned studies have demonstrated comparable adsorption behaviours at low pressures, which are much in line with the values reported in this work. Post-synthetic modification of ZTCs is anticipated to enhance their textural properties, which may, in turn, lead to an improvement in hydrogen adsorption capacity [13, 37, 39].

8 Conclusions

The study has demonstrated that utilisation of biogas in its raw form does not lead to the production of ZTCs due to competition of CO_2 during the CVD process. However, when pure methane (in this case simulated 'biomethane') was utilised, the ZTCs obtained were almost similar to those obtained using commercial ethylene gas feedstock. When the one-step process was followed (using CH_4 only), the surface area of the obtained ZTCs (2015 m^2/g) was lower than the surface area of the two-step process (2974 m^2/g) that utilised prior impregnation of furfural alcohol followed by CH_4. The two-step carbons demonstrated enhanced hydrogen uptake capacities, particularly under low-pressure conditions, due to the abundance of microporous adsorption sites. The morphology of all the obtained ZTCs was a close replica of the parent zeolite. Furthermore, we demonstrated complete template removal through TGA analysis (i.e., weight loss of ~99% at 900 °C). Noteworthy is that the study has, for the first time, demonstrated the potential for the value addition of biogas (after upgrading) through the development of a new product stream (ZTC).

Author contributions

KM: ** Investigation, Formal Analysis, Writing-originalXD: ** Data analysis, Visualisation, Review & Editing**HWL: ** Supervision, Funding acquisition, Review & Editing**NMM: ** Conceptualisation, Supervision, Funding acquisition, Review & Editing.

Funding

The authors of this paper would like to acknowledge the financial support from Future Leaders – African Independent Research (FLAIR) Fellowship (Grant ref: FLR\R1\201528) for NM Musyoka, the Council for Scientific and Industrial Research (CSIR) and the Nottingham Ningbo China Beacons of Excellence Research and Innovation Institute for extended support. HWL acknowledges the South African Research Chairs Initiative (SARChI) of the Department of Science and Innovation (DSI) and the National Research Foundation (NRF) (Grant Number: 150526). Any opinions, findings and/or recommendations expressed here are those of the authors and not of the funding bodies.

Data availability

Data will be made available on request with the corresponding author.

Declarations

Ethics approval and consent to participate

Not applicable.

Consent for publication

Not applicable.

Competing interests

The authors declare no competing interests.

Received: 19 May 2025 / Accepted: 29 October 2025
Published online: 24 November 2025

References

1. Kougias PG, Angelidaki I. Biogas and its opportunities—A review. Front Environ Sci Eng. 2018;12:1–12.
2. Okonkwo UC, Onokpite E, Onokwai AO. Comparative study of the optimal ratio of biogas production from various organic wastes and weeds for digester/restarted digester. J King Saud University-Engineering Sci. 2018;30(2):123–9.
3. Surendra K, Takara D, Hashimoto AG, Khanal SK. Biogas as a sustainable energy source for developing countries: opportunities and challenges. Renew Sustain Energy Rev. 2014;31:846–59.
4. Guan R, Yuan H, Yuan S, Yan B, Zuo X, Chen X, Li X. Current development and perspectives of anaerobic bioconversion of crop stalks to biogas: A review. Bioresour Technol. 2022;349:126615.
5. Rosha P, Rosha AK, Ibrahim H, Kumar S. Recent advances in biogas upgrading to value added products: A review. Int J Hydrog Energy. 2021;46(41):21318–37.
6. Golmakani A, Nabavi SA, Wadi B, Manovic V. Advances, challenges, and perspectives of biogas cleaning, upgrading, and utilisation. Fuel. 2022;317:123085.
7. Mofarahi M, Bakhtyari A. Experimental investigation and thermodynamic modeling of CH4/N2 adsorption on zeolite 13X. J Chem Eng Data. 2015;60(3):683–96.
8. Cavenati S, Grande CA, Rodrigues AE. Adsorption equilibrium of methane, carbon dioxide, and nitrogen on zeolite 13X at high pressures. J Chem Eng Data. 2004;49(4):1095–101.
9. Silva JA, Schumann K, Rodrigues AE. Sorption and kinetics of CO2 and CH4 in binderless beads of 13X zeolite. Microporous Mesoporous Mater. 2012;158:219–28.
10. Bermeo M, Vega LF, Abu-Zahra MR, Khaleel M. Critical assessment of the performance of next-generation carbon-based adsorbents for CO2 capture focused on their structural properties. Sci Total Environ. 2022;810:151720.
11. Kwon HC, Choi S, Wang Y, Othman R, Choi M. Scalable synthesis of zeolite-templated ordered microporous carbons without external carbon deposition for capacitive energy storage. Microporous Mesoporous Mater. 2020;307:110481.
12. Kyotani T, Ma Z, Tomita A. Template synthesis of novel porous carbons using various types of zeolites. Carbon. 2003;41(7):1451–9.
13. Xia Y, Yang Z, Mokaya RCVD. Nanocasting routes to Zeolite-Templated carbons for hydrogen storage. Chem Vap Deposition. 2010;16(10–12):322–8.
14. Liu Y, Osta EH, Poryvaev AS, Fedin MV, Longo A, Nefedov A, Kosinov N. Direct conversion of methane to zeolite-templated carbons, light hydrocarbons, and hydrogen. Carbon. 2023;201:535–41.
15. Gaslain FO, Parmentier J, Valtchev VP, Patarin J. First zeolite carbon replica with a well resolved X-ray diffraction pattern. Chem Commun 2006, (9), 991–3.
16. Musyoka NM, Ren J, Langmi HW, North BC, Mathe M. A comparison of hydrogen storage capacity of commercial and fly ash-derived zeolite X together with their respective templated carbon derivatives. Int J Hydrog Energy. 2015;40(37):12705–12.
17. Yang Z, Xia Y, Sun X, Mokaya R. Preparation and hydrogen storage properties of zeolite-templated carbon materials nanocast via chemical vapor deposition: effect of the zeolite template and nitrogen doping. J Phys Chem B. 2006;110(37):18424–31.
18. Stadie NP, Vajo JJ, Cumberland RW, Wilson AA, Ahn CC, Fultz B. Zeolite-templated carbon materials for high-pressure hydrogen storage. Langmuir. 2012;28(26):10057–63.
19. Annamalai P, Musyoka NM, Ren J, Langmi HW, Mathe M, Bessarabov D, Petrik LF. Electrospun zeolite-templated carbon composite fibres for hydrogen storage applications. Res Chem Intermed. 2017;43:4095–102.
20. Choi S, Alkhabbaz MA, Wang Y, Othman RM, Choi M. Unique thermal contraction of zeolite-templated carbons enabling micropore size tailoring and its effects on methane storage. Carbon. 2019;141:143–53.
21. Stadie NP, Murialdo M, Ahn CC, Fultz B. Anomalous isosteric enthalpy of adsorption of methane on zeolite-templated carbon. J Am Chem Soc. 2013;135(3):990–3.
22. Antoniou MK, Diamanti EK, Enotiadis A, Policicchio A, Dimos K, Ciuchi F, Maccallini E, Gournis D, Agostino RG. Methane storage in zeolite-like carbon materials. Microporous Mesoporous Mater. 2014;188:16–22.
23. Gholipour F, Mofarahi M. Adsorption equilibrium of methane and carbon dioxide on zeolite 13X: experimental and thermodynamic modeling. J Supercrit Fluids. 2016;111:47–54.
24. Pour AA, Sharifnia S, NeishaboriSalehi R, Ghodrati M. Performance evaluation of clinoptilolite and 13X zeolites in CO2 separation from CO2/CH4 mixture. J Nat Gas Sci Eng. 2015;26:1246–53.
25. Kareem FAA, Shariff A, Ullah S, Mellon N, Keong L. Adsorption of pure and predicted binary (CO2: CH4) mixtures on 13X-Zeolite: equilibrium and kinetic properties at offshore conditions. Microporous Mesoporous Mater. 2018;267:221–34.
26. Mulgundmath V, Tezel F, Saatcioglu T, Golden T. Adsorption and separation of CO2/N2 and CO2/CH4 by 13X zeolite. Can J Chem Eng. 2012;90(3):730–8.
27. Kyotani T, Nagai T, Inoue S, Tomita A. Formation of new type of porous carbon by carbonization in zeolite nanochannels. Chem Mater. 1997;9(2):609–15.
28. Nishihara H, Yang Q-H, Hou P-X, Unno M, Yamauchi S, Saito R, Paredes JI, Martínez-Alonso A, Tascón JM, Sato Y. A possible buckybowl-like structure of zeolite templated carbon. Carbon. 2009;47(5):1220–30.
29. Leyva-García S, Nueangnoraj K, Lozano-Castello D, Nishihara H, Kyotani T, Morallón E. Cazorla-Amorós, D. Characterization of a zeolite-templated carbon by electrochemical quartz crystal microbalance and in situ Raman spectroscopy. Carbon. 2015;89:63–73.
30. Bokobza L, Bruneel J-L, Couzi M. Raman spectroscopy as a tool for the analysis of carbon-based materials (highly oriented pyrolitic graphite, multilayer graphene and multiwall carbon nanotubes) and of some of their elastomeric composites. Vib Spectrosc. 2014;74:57–63.
31. Lee S-K, Park H, Yoon JW, Kim K, Cho SJ, Maurin G, Ryoo R, Chang J-S. Microporous 3D graphene-like zeolite-templated carbons for Preferential adsorption of Ethane. ACS Appl Mater Interfaces. 2020;12(25):28484–95.

32. Lowell S, Shields JE, Thomas MA, Thommes M. Characterization of porous solids and powders: surface area, pore size and density. Springer Science & Business Media; 2012.
33. Song X, Xu R, Wang K. The structural development of zeolite-templated carbon under pyrolysis. J Anal Appl Pyrol. 2013;100:153–7.
34. Musyoka NM, Ren J, Annamalai P, Langmi HW, North BC, Mathe M, Bessarabov D. Synthesis of a hybrid MIL-101 (Cr)/ZTC composite for hydrogen storage applications. Res Chem Intermed. 2016;42:5299–307.
35. Masika E, Mokaya R. Preparation of ultrahigh surface area porous carbons templated using zeolite 13X for enhanced hydrogen storage. Progress Nat Science: Mater Int. 2013;23(3):308–16.
36. Cai J, Li L, Lv X, Yang C, Zhao X. Large surface area ordered porous carbons via Nanocasting zeolite 10X and high performance for hydrogen storage application. ACS Appl Mater Interfaces. 2014;6(1):167–75.
37. Sevilla M, Alam N, Mokaya R. Enhancement of hydrogen storage capacity of zeolite-templated carbons by chemical activation. J Phys Chem C. 2010;114(25):11314–9.
38. Xia Y, Mokaya R, Grant DM, Walker GS. A simplified synthesis of N-doped zeolite-templated carbons, the control of the level of zeolite-like ordering and its effect on hydrogen storage properties. Carbon. 2011;49(3):844–53.
39. Musyoka NM, Rambau KM, Manyala N, Ren J, Langmi HW, Mathe MK. Utilization of waste tyres pyrolysis oil vapour in the synthesis of zeolite templated carbons (ZTCs) for hydrogen storage application. J Environ Sci Health Part A. 2018;53(11):1022–8.

Publisher's note